npj | Quantum Information

www.nature.com/npjqi

ARTICLE OPEN

Check for updates

Suppression of nuclear spin fluctuations in an InGaAs quantum dot ensemble by GHz-pulsed optical excitation

E. Evers[1✉], N. E. Kopteva[1], I. A. Yugova[2], D. R. Yakovlev[1,3], D. Reuter[4,5], A. D. Wieck[4], M. Bayer[1,3] and A. Greilich[1]

The coherent electron spin dynamics of an ensemble of singly charged (In,Ga)As/GaAs quantum dots in a transverse magnetic field is driven by periodic optical excitation at 1 GHz repetition frequency. Despite the strong inhomogeneity of the electron *g* factor, the spectral spread of optical transitions, and the broad distribution of nuclear spin fluctuations, we are able to push the whole ensemble of excited spins into a single Larmor precession mode that is commensurate with the laser repetition frequency. Furthermore, we demonstrate that an optical detuning of the pump pulses from the probed optical transitions induces a directed dynamic nuclear polarization and leads to a discretization of the total magnetic field acting on the electron ensemble. Finally, we show that the highly periodic optical excitation can be used as universal tool for strongly reducing the nuclear spin fluctuations and preparation of a robust nuclear environment for subsequent manipulation of the electron spins, also at varying operation frequencies.

npj Quantum Information (2021)7:60 ; https://doi.org/10.1038/s41534-021-00395-1

INTRODUCTION

The last decade has been marked by unprecedented progress in the development of quantum technologies. This is confirmed by the development and first implementation of quantum communication[1] and quantum computing[2]. At the heart of these technologies are solid state quantum bits (qubits) and their entanglement[3]. As the race for the best qubit candidate is still ongoing, it becomes clear that there will be no monolithic solution, but rather a hybrid solution combining different excitations, each exploiting its own best property while contributing to the common goal of the targeted quantum technology.

One of the possible hybrid qubit realizations is the spin of an electron confined in a semiconductor quantum dot (QD), which is interacting with the surrounding nuclear spins[3]. The prominent advantage of QDs is their strong optical dipole moment, which allows efficient coupling of photons to the confined electron spins, according to optical selection rules. The electron spin is coupled to the nuclear spins of the QD crystal lattice by the hyperfine interaction[4], which could allow one to design schemes where the angular momentum of the photon is transferred to the nuclear spins using the electron spin as auxiliary state. The advantage of this approach is that the electron spin coherence is limited to several microseconds at low temperatures[5], but the nuclear spin coherence can last milliseconds[6], allowing in particular the implementation of quantum repeater schemes[7].

The idea to transfer the electron spin state to the surrounding nuclear spins is aggravated by the intrinsic nuclear spin fluctuations[4]. A way to reduce these fluctuations was first elaborated theoretically[8] and later demonstrated in a series of experiments[9–13]. Further advancement in the reduction of nuclear spin fluctuations led to the possibility to implement all-optical access to the individual quantized transitions of the strongly coupled electron-nuclear spin systems[14]. All these experiments were realized on single QDs and required a high spectral precision.

In this paper, we explore an alternative and universal tool that has relaxed requirements on spectral and other material contents-related differences of single QDs. Using a single pulsed laser source it becomes possible to control the state of all QDs whose optical transitions fall into the spectrum of the laser at the same time. To prove its universality, we apply our method to an ensemble of QDs and detect their joint response. We expose this inhomogeneous ensemble of singly-charged (In,Ga)As/GaAs QDs to a high repetition laser operated at 1 GHz rate. Exploiting the strong electron-nuclear feedback we drive the inhomogeneous ensemble of electron spins into single frequency Larmor precession about a transverse magnetic field. Additionally, we demonstrate the discretization of the total magnetic field acting on the electron spin ensemble and demonstrate a reduction of the nuclear spin fluctuations, which leads to a deceleration of the electron spin dephasing. We further demonstrate that one can prepare the QD system using a high repetition rate excitation in such a low dephasing-state and then switch non-detrimentally to another laser source operating at a different repetition frequency for subsequent manipulation. This can be done on time scales up to seconds to continue manipulation of the electron spins in the reduced fluctuation environment.

RESULTS

Prolongation of the spin dephasing time T_2^*

An ensemble of self-assembled QDs is known to be intrinsically inhomogeneous. Figure 1a shows an atomic force microscopy image of the studied QD ensemble, from which the variation of the QD sizes becomes apparent. This inhomogeneity leads to the broad emission spectrum shown by the light gray shaded trace in Fig. 1b. Furthermore, every QD in the ensemble contains about 10^5 nuclear spins, so that one expects nuclear-spin fluctuations in the Overhauser field (δB_N)[4,15] acting on the electron spins in the QDs due to the hyperfine interaction, see sketches in Fig. 1a. Due

[1]Experimentelle Physik 2, Technische Universität Dortmund, 44221 Dortmund, Germany. [2]Spin Optics Laboratory, St. Petersburg State University, 198504 St. Petersburg, Russia. [3]Ioffe Institute, Russian Academy of Sciences, 194021 St. Petersburg, Russia. [4]Angewandte Festkörperphysik, Ruhr-Universität Bochum, 44780 Bochum, Germany. [5]Present address: Department Physik, Universität Paderborn, 33098 Paderborn, Germany. ✉email: eiko.evers@tu-dortmund.de

Published in partnership with The University of New South Wales

npj nature partner journals

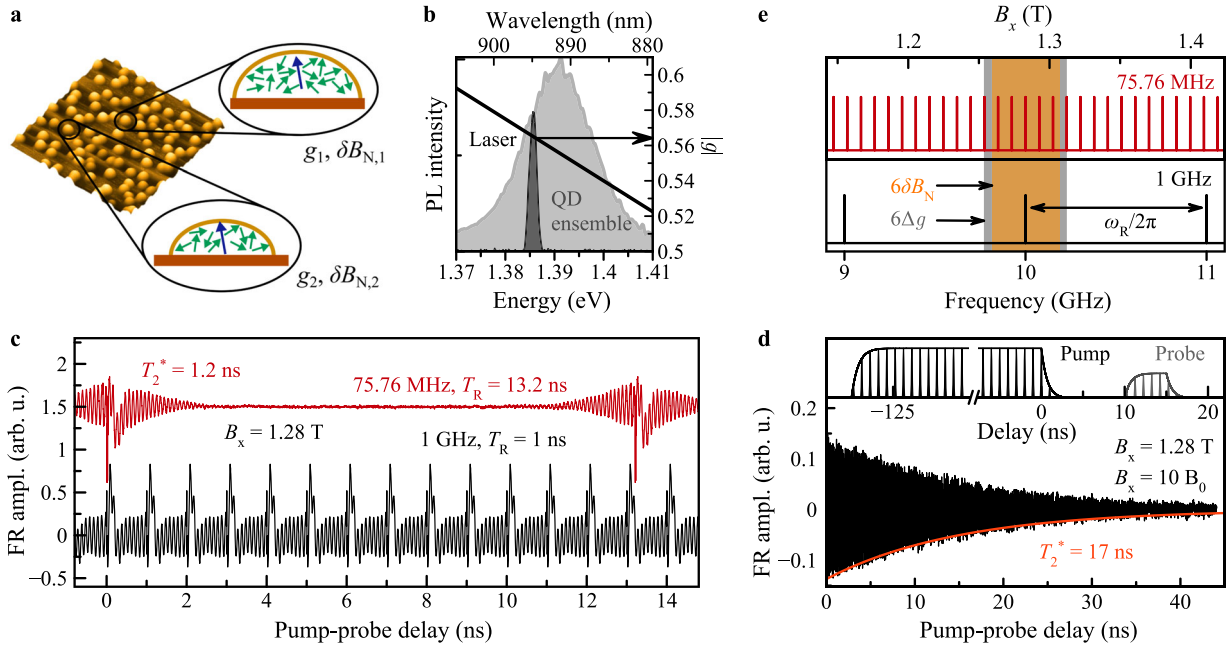

Fig. 1 Dependence of spin dephasing time T_2^* on laser repetition frequency. a Atomic force microscope of the (In,Ga)As/GaAs QD ensemble with a QD density of 10^{10} cm^{-2}. Sketches indicate the nuclear spins (green arrows) interacting with a single electron (blue arrow). The QDs differ in size as well as in g-factor value. **b** Photoluminescence (PL) spectrum of the (In,Ga)As/GaAs QD ensemble (light gray) and spectrum of the picosecond laser emission, shown by the dark gray shaded profile. The black line gives the dispersion of the absolute electron g factor. **c** Time-resolved Faraday rotation for laser repetition frequencies of 75.76 MHz (red) and 1 GHz (black). **d** Extended pump-probe signal with $T_2^* = 17$ ns. The inset shows the sequences of the applied pump and probe pulse bunches. For panels **c** and **d** containing experimental data the following conditions hold: $T = 5.3$ K, $E_{Pu/Pr} = 1.3867$ eV. Used laser powers: for 75.76 MHz $P_{Pu} = 600$ W/cm^2, $P_{Pr} = 6$ W/cm^2; for 1 GHz $P_{Pu} = 260$ W/cm^2, $P_{Pr} = 8$ W/cm^2. **e** Scheme of the PSC fulfilling precession frequencies (red lines) for the 75.76 MHz laser. The orange area shows the spread of the nuclear fluctuations in the QDs, $6\delta B_N = 45$ mT, and the gray shaded area gives the precession frequency range due to g-factor spread at $B_x = 1.28$ T. The black lines below demonstrate the situation for the 1 GHz laser excitation. Here, the mode separation is increased to 128 mT.

to the variation of the constituent material, the inhomogeneity is also present in the electron g factors in the ensemble, whose dispersion is shown by the black line in Fig. 1b. The combination of these effects manifests itself as a fast dephasing of the measured ensemble spin dynamics in magnetic field, occuring on the timescale T_2^* of a nanosecond[5,16]. These inhomogeneities can, however, be overcome by the experiment's design, exploiting the effects of spin mode-locking (SML)[5] and nuclear induced frequency focusing (NIFF)[17,18].

To study the coherent spin dynamics in the QD ensemble, we use time-resolved Faraday rotation (FR). Exemplary traces for pulsed excitation with repetition frequencies of 75.76 MHz (red) and 1 GHz (black), corresponding to repetition periods of $T_R = 13.2$ ns and $T_R = 1$ ns, respectively, are shown in Fig. 1c for $B_x = 1.28$ T. As one can see, for the case of $T_R = 13.2$ ns the signal decays within $T_2^* = 1.2$ns, while there is no observable spin decay for 1 ns pulse separation. Here, an assessment of the temporal dynamics is impossible for times exceeding 1 ns, therefore we apply an adapted extended pump-probe method[19]. The spin dynamics is shown in Fig. 1d, demonstrating electron spin dephasing on a timescale of $T_2^* = 17$ns. In this case, pump and probe pulses are picked by electro-optical modulators and hit the sample in bunches, with a controlled delay time between the pump and probe pulse combinations, see the inset in Fig. 1d. Additional data can be found in the Supplementary Note 1.

To explain the observed difference in T_2^* for both repetition frequencies, we first consider the case of 13.2 ns repetition period. The FR signal exhibits a pronounced rise of the electron spin polarization before each pump pulse arrival (0 ns or 13.2 ns delay) which mirrors the decay thereafter (effect of SML)[5]. Both the decay and the rise of the signal are caused by the superposition of multiple precession modes which leads to destructive signal interference between the pump pulses. At a delay of a multiple integer of T_R, constructive interference occurs for particular modes with discrete electron spin precession frequencies ω. Generally, $\omega = g\mu_B B_x/\hbar$ in the external magnetic field B_x, where μ_B is the Bohr magneton and $\hbar$ is the reduced Planck constant. The frequencies of the constructively interfering precession modes satisfy the phase synchronization condition (PSC) $\omega = K\omega_R$, where $\omega_R = 2\pi/T_R$ is the repetition rate of the laser pulses and K is an integer characterizing each contributing mode. As discussed in refs. [20,21], the number of PSC precession modes, M, within the inhomogeneous ensemble is given by: (1) the g-factor spread of the optically excited electron spins (Δg), (2) the nuclear spin fluctuations (δB_N), (3) the external magnetic field (B_x), and (4) the laser repetition period T_R.

The black solid line in Fig. 1b demonstrates the dependence of the electron g factor on the optical excitation energy, following roughly a linear dependence with a slope of $\Delta g/\Delta E = -1.75$ eV^{-1}[22,23]. Using the laser energy and the spectral pulse width, this dependence allows us to determine the average g factor at the probe energy of 1.3867 eV to be $|g| = 0.57$ with a spread of $\Delta g = 0.004$[24]. The nuclear field fluctuations are known to be $\delta B_N = 7.5$ mT for this sample[20]. Therefore, the number of contributing PSC modes at $B_x = 1.28$ T is dominated by the g-factor spread which covers $M = 8$ modes for $T_R = 13.2$ ns, as shown by the gray-shaded area in Fig. 1e[25].

The number of modes M is derived here for a width of the Gaussian precession frequency distribution taken as six times its half width at half maximum (HWHM), to account for 99.7% of the spins[25]:

$$M = 6\Delta\omega T_R/2\pi, \quad (1)$$

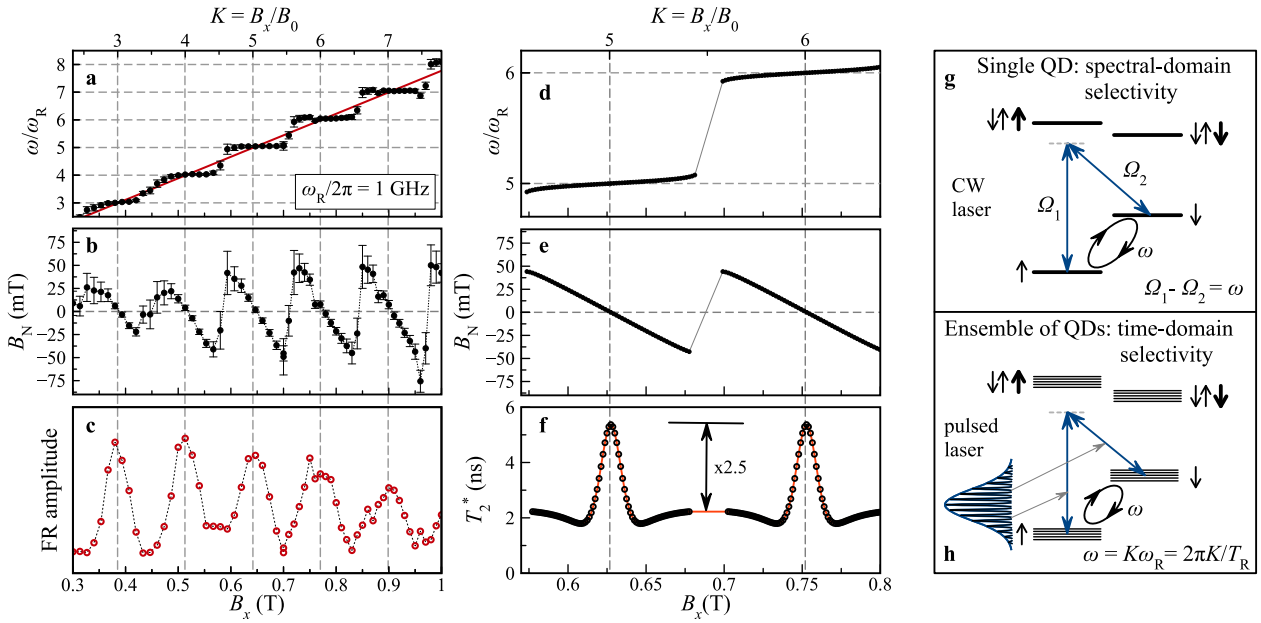

Fig. 2 Discretization of precession frequency by nuclear polarization. a Electron precession frequency in units of repetition frequency of the laser vs. external magnetic field in absolute units (lower axis) and in units of $B_0 = 128$ mT (upper axis) - the black dots. Error bars give the frequency fitting error with Eq. (3). Red line shows the electron precession frequency dependence on the magnetic field without the contribution of nuclear spin polarization. **b** Overhauser-field dependence on external magnetic field. The dotted line is a guide to the eye. **c** Amplitude of the Faraday rotation signal measured vs. B_x. The data in panels **a**-**c** are measured for a negative pump-probe spectral detuning: $E_{Pu} = 1.3839$ eV and $E_{Pr} = 1.3864$ eV. **d** Modeling of the frequency dependence on the external magnetic field. Plateaus around the modes 5 and 6 are clearly observable. **e** Magnetic field dependence of Overhauser-field built up in the QDs for compensation of the external field. **f** Variation of the spin dephasing time with external magnetic field. The multiplication factor of 2.5 is expected based on the simulation parameters. **g** Schematics of the energy levels of a singly charged QD in Voigt geometry and the two lasers photon energies $\hbar\Omega_1$ and $\hbar\Omega_2$, slightly detuned from the trion transitions, driving the Λ system for coherent population trapping. ω is the Larmor frequency. **h** Ensemble of singly charged QDs driven by a negatively detuned pulsed excitation in the Voigt geometry. The laser pulse can be represented as a frequency comb combining multiple CW frequencies that satisfy the CPT for QDs having different optical transition energies and g factors. We highlight a pair of CW laser components by gray arrows for one contributing QD. An alternative explanation is also given in the main text.

where

$$\Delta\omega = \mu_B \sqrt{(\Delta g B_x)^2 + (g\delta B_N)^2}/\hbar. \quad (2)$$

The nuclear fluctuation field δB_N shown by the orange-shaded area is dominant only at small magnetic fields[20], where Δg does not contribute significantly anymore. For $T_R = 13.2$ ns, the number of modes covered by the frequency distribution is larger than unity for any magnetic field strength, causes generally fast spin dephasing.

The situation for 1 GHz laser repetition rate is shown by the black trace in Fig. 1c. For pulsed excitation with $T_R = 1$ ns, the separation between neighboring PSC modes is $B_0 = \hbar\omega_R/(g\mu_B) = 128$ mT, which is much larger than the δB_N of the nuclear spin fluctuations (7.5 mT). Moreover, the g-factor spread is also not sufficient to allow for more than one mode within the 128 mT range at a field of $B_x = 1.28$ T (see the black lines in Fig. 1e). As a result, the signal shows a single, slowly decaying oscillation with $T_2^* = 17$ ns instead of a multi-mode signal with a fast dephasing time of 1 ns. Hence, the pump-probe signal between two pump pulses for 1 GHz excitation can be evaluated using a single cosine function with a frequency ω:

$$S(t) = S_1 \cos(\omega t). \quad (3)$$

S is the signal amplitude, $S_1 = S_0 \exp(-t/T_2^*)$ where S_0 is the electron spin polarization created by the pump, t is the pump-probe time delay and T_2^* is the electron spin dephasing time related to the single-mode frequency bandwidth.

Influence of nuclear spins

As the next step, due to the time-resolution limitations set by the electronics in the extended pump-probe scheme, we use the common pump-probe protocol and fit Eq. (3) to the FR data taken for different external magnetic fields (B_x) for 1 GHz excitation. S_1 is considered to be time independent here as $T_2^* \gg T_R = 1$ ns. The oscillation frequency should depend linearly on the external magnetic field, as shown in Fig. 2a by the red line. The data of the Larmor frequency evaluated by Eq. (3) are shown by the black dots in Fig. 2a, and demonstrate a non-linear step-like dependence of ω, normalized by the laser repetition rate ω_R.

As one can see in Fig. 2a, the electron spin precession frequency shows small deviations from the linear dependence in small magnetic fields ($B_x < 0.5$ T). Increasing the magnetic field leads to the appearance of pronounced plateaus in the frequency dependence. The positions of the plateaus are fixed by the PSC on integer numbers of full spin revolutions during T_R or $\omega = K\omega_R$. The center of each plateau corresponds to $B_x = KB_0$ (the upper axis in Fig. 2a). The origin of this dependence is related to a nuclear magnetic field (B_N) resulting from the mean value of the Overhauser field exerted by the dynamically polarized nuclear spins, acting on the electron spin in each dot. Depending on the external magnetic field, B_N decreases or increases the total magnetic field seen by the electron. The subtraction of the linear dependence from the experimental data allows us to extract the amplitude of B_N as function of B_x. One can see in Fig. 2b that the maximal amplitude of B_N reaches 50 mT and can be oriented parallel or anti-parallel to the external field.

Such plateaus in the dependence of the electron spin precession frequency on the external magnetic field were observed earlier for electron spins localized on Fluorine donors

in ZnSe epilayers[26]. One can explain them in terms of a dynamic nuclear polarization in the following way: the non-resonant optical excitation of the trion resonance leads to the appearance of an effective magnetic field along the light propagation direction - the optical Stark field. This field is perpendicular to B_x, the electron spin precesses about the total magnetic field which is tilted relative to the x-axis. This leads to the appearance of a sizable component of electron spin polarization along the x-axis (S_x), which efficiently polarizes the nuclear spins along the external magnetic field B_x[27,28]. The nuclear polarization plays the role of the additional field described in the previous paragraph – the Overhauser field, which acts back on the electron spins[29,30].

In the experiments presented in Fig. 2, we use a negative optical detuning, where the energy of the probe at the trion resonance is higher than the pump excitation energy[23,27]. For a negative optical detuning in combination with the negative sign of the electron g factor in the (In,Ga)As QDs, the Overhauser field adds to the external B_x for electron spins which do not satisfy the PSC, driving their frequency to the PSC-consistent value, i.e. a laser period-commensurate value. This leads to the plateau-like behavior seen in Fig. 2a. The Overhauser field B_N reaches the maximal amplitude of about 50 mT when the external field is slightly larger than $B_x = 0.5KB_0$ (see Fig. 2b). Its amplitude decreases with increasing B_x and becomes zero at $B_x = KB_0$, the center of the plateau. A further increase of B_x changes the direction of B_N. Here, it reaches the maximal negative amplitude slightly below $B_x = 0.5KB_0$.

Figure 2c demonstrates the value of S_1 in Eq. (3) determined from the fits to the data as function of B_x, demonstrating a strong modulation. The magnetic field positions of the peaks correspond to integer spin precession periods within T_R, i. e. to fulfilled PSC. This allows us to assume that the T_2^* time should be similarly modulated, as the amplitude S_0 in Eq. (3) is expected to stay constant across the plateau, due to the constant values of the Larmor frequencies. To understand this behavior we use the theory presented in ref. [28], which relates the extension of the spin dephasing time at the plateau centers to the feedback strength between the electron and nuclear systems, and to the reduction of the nuclear spin fluctuations (the variance of the Overhauser field) (see Supplementary Note 4 and Supplementary Note 5 for more details).

Figure 2d demonstrates the simulation of the frequency behavior (normalized by the laser repetition frequency ω_R) as a function of the external magnetic field B_x. The bottom scale gives the applied field, while the top one is normalized by the mode separation B_0. One finds fully developed plateaus around the modes 5 and 6. Figure 2e shows the Overhauser field B_N building up in the QD system as function of B_x. The parameters of the modeling are given in the Supplementary Note 5.

As suggested in ref. [26], for the electron spins satisfying the PSC the strong feedback should lead to a reduction of the nuclear spin fluctuations and, as a result, the spin dephasing time of the ensemble T_2^* should be prolonged. As soon as B_x differs from $B_x = KB_0$, the nuclear fluctuations recover due to the reduced feedback strength (see Supplementary Note 5). The dynamical nuclear polarization process looses its efficiency, even though the x-component of the electron spin polarization is largest for $B_x = 0.5KB_0$. At this field ($B_x = 0.5KB_0$), the amplitude of B_N becomes redirected within a relatively narrow magnetic field interval.

The magnetic field variation of the spin dephasing time T_2^* calculated by Eqs. (1)–(6) in the Supplementary Note 5, is demonstrated in Fig. 2f. Depending on the magnetic field, this time becomes strongly modulated due to the periodic changes of the amplitude of the nuclear fluctuations. For the parameters used in our modeling, we expect a prolongation of the T_2^* time by a factor of 2.5.

The process of reduction of the nuclear field fluctuations at the center of the plateaus without build-up of nuclear polarization can be qualitatively understood in a similar way as the process of coherent population trapping (CPT) suggested for a single QD[8,9,12,28,31]. As a reminder, once the difference of the photon energies of two linearly polarized continuous wave (CW) lasers Ω_1 and Ω_2 is equal to the Zeeman splitting of the ground state electron spin (↑ and ↓), the system goes into a coherent dark state without the possibility of photon scattering into the excited trion state, see Fig. 2g. Due to the nuclear spin fluctuations, the electron Zeeman splitting varies, moving the system out of the dark state. This leads to enhanced driving of one of the two optical transitions that causes scattering of photons and pulls the Zeeman splitting back to that of the dark state by changing the nuclear spin orientation in the surrounding. Such locking into the dark state induces the reduced variance of the Overhauser field.

In the case of pulsed excitation, as we use in our demonstration, the situation of reduction of the nuclear fluctuations can be seen in a similar way. However, in this case a short laser pulse can be presented as a combination of many CW lasers (frequency comb) with different frequencies. Therefore, there is a set of different two-frequency-combinations (Ω_1 and Ω_2) separated by different electron Larmor frequencies[28]. These combinations can satisfy the CPT conditions for different QDs with corresponding spread of trion transitions, present in an inhomogeneous ensemble of QDs, see Fig. 2h. Furthermore, one can represent the process of periodical pulsed excitation in an alternative way. In the transverse magnetic field, the pulsed circular excitation leads to creation of a coherent superposition of the ground state spin states (shown by the multiple lines for the ensemble). This superposition precesses in the magnetic field at the Larmor frequency $\omega = g\mu_B B_x/\hbar$. When this frequency is commensurate to the laser repetition frequency $\omega_R = 2\pi K/T_R$, the efficiency of spin polarization is strongly enhanced[24]. Once the electron spin oscillates at one of these frequencies, it can also be seen as locked in a coherent dark state, as the Pauli principle forbids further excitation of the spin by circularly polarized pulses. If the nuclear field fluctuations bring the Zeeman splitting (or the Larmor frequency) out of the resonance condition, the interaction with the nuclear surrounding pulls the frequency back to the dark state, leading similarly to a reduction of the variance of the Overhauser field[17,27]. In comparison to CW lasers, the pulsed excitation allows us to excite a spectrally broad distribution of QD transitions and can be seen as universal tool without strict requirement concerning the excitation laser energies for spectrally different QDs.

Two-laser protocol

The relaxation dynamics of the contributing electron and nuclear spins differ by several orders of magnitude. The spin lifetime (T_1) of the resident electrons in the studied QDs was previously measured, reaching 1.7 μs[32], while the lifetime of the nuclear spins for this sample ranges from several seconds under laser illumination up to hours in darkness[17]. We want to make use of this difference and implement a protocol that suppresses the nuclear fluctuations by the 1 GHz excitation and subsequently allows us to manipulate the electron spins with an arbitrary laser source in the prepared nuclear environment. Supplementary Note 2 shows such an implementation of the suggested alternating driving by the two available lasers. At this point we note, that in our experiment, the reduction of nuclear spin fluctuations is still present at the timescale of seconds without driving the system by the GHz laser. This observation seems to contradict previous experiments in single QDs, where the prepared state with reduced nuclear fluctuations decays with 46 ms[12]. However, as measurements of the same group demonstrate, for the nuclear system with reduced nuclear fluctuations (variance) and increased nuclear polarization (mean value of the Overhauser field) the relaxation

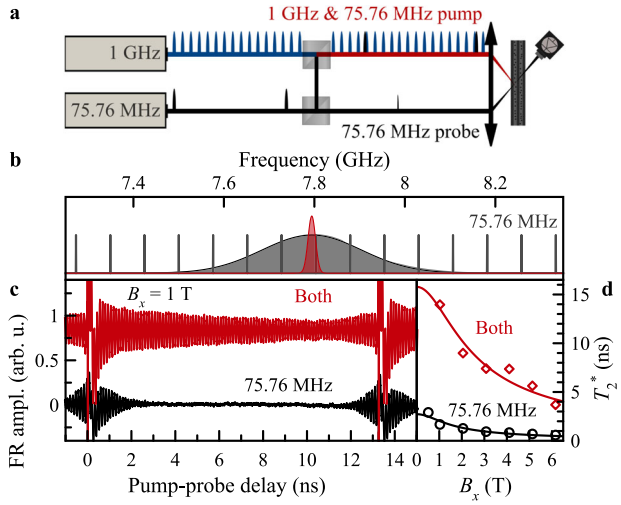

Fig. 3 Two-lasers protocol. a Schematics of the protocol with two lasers applied to the same ensemble of QDs. The pump pulses of both lasers are applied simultaneously, while only the 75.76 MHz laser probes the sample. **b** PSC modes for the 75.76 MHz excitation with the frequency distributions in the unexcited ensemble of electrons, covering 7 modes for $B_x = 1$ T (black) and for the 1 GHz excited ensemble, covering only a single PSC mode (red). **c** Pump-probe traces for the 75.76 MHz case (black) and for both lasers applied (red) at $B_x = 1$ T. **d** The spin dephasing time T_2^* determined for the case without the 1 GHz laser illumination (black) and with the 1 GHz laser (red) vs. magnetic field. Lines are fits using Eq. (4). All lasers are degenerate at $E_{Pu/Pr} = 1.3867$ eV.

becomes biexponential with longer times reaching seconds[33]. It demonstrates that the difference in the relaxation times might depend on how the nuclear system is prepared, which requires further investigations.As the measurement with alternating lasers takes a long time for the experiments (about 3 hours for one temporal trace), we present here an alternative realization of this idea.

Figure 3a demonstrates a scheme, in which both lasers (75.76 MHz and 1 GHz) are applied simultaneously to the same QD ensemble. In this case we measure a pump-probe trace using the 75.76 MHz laser while pump pulses of the 1 GHz laser simultaneously excite the same ensemble, without any synchronization between the lasers. Figure 3c demonstrates a comparison between the case when only the 75.76 MHz laser is applied (black) and the situation with both lasers (red). As one can see, in the latter case the dephasing of the ensemble is strongly reduced, which is a direct demonstration of a strong reduction of the frequency spread compared with the pure 75.76 MHz case. As the emissions of the two lasers are not synchronized to each other, the Faraday rotation measured by the probe pulses only stems from the electron spins oriented by the pump pulses with the repetition period of 75.76 MHz. There is still some minor mode-locking signal, as seen by the weak signal increase before the pump at 13.2 ns, which might arise from the QDs not excited by the GHz laser. The sketch in Fig. 3b demonstrates the calculated mode distributions for both cases, with the corresponding changes in the frequency distributions of the ensemble given by the spreads Δg and δB_N, the colors correspond to the traces in Fig. 3c.

Using the two-laser approach we measure the magnetic field dependence of T_2^* for the two cases, using only the 75.76 MHz laser and using both lasers applied. Figure 3d demonstrates such a measurement, where the pump-probe traces are measured at the center of plateaus for a set of magnetic fields. For the analysis of these traces we took into account that the signal of a single mode oscillation for the two-laser approach can interfere with the multi-mode signal from the 75.76 MHz laser applied alone (see Supplementary Note 3 for a detailed trace analysis).

We characterize the dephasing behavior of the extracted signal using the form:

$$T_2^* = \hbar / \left[\mu_B \sqrt{(\Delta g B)^2 + (g \delta B_N)^2} \right]. \quad (4)$$

This leads to the following fit values: (i) 75.76 MHz only, $\Delta g = 4 \times 10^{-3}$, $\delta B_N = 7.5$ mT and (ii) both lasers, $\Delta g = 4.2 \times 10^{-4}$, $\delta B_N = 1.3$ mT. The reduction of the g-factor dispersion by one order of magnitude can be explained by the reduction of the frequency spread to a single mode, which is also additionally reduced in width by the NIFF. The reduction of the nuclear fluctuations δB_N for the whole QD ensemble can be extracted from the width extrapolated to $B_x = 0$ and gives a factor of 5.8, which is comparable to the value of 12 achieved in optimal conditions for a single QD, using the coherent population trapping technique[12]. Note that our experiment demonstrates a higher reduction than the factor 2.5 suggested by our model calculation, see Fig. 2f. Taking into account the simplicity of the model, based purely on the optical Stark effect[26,34] and collinear hyperfine interaction[15], it still gives a good estimate. Another approach, using the collinear hyperfine interaction, is presented by ref. [35], demonstrating optimal reduction of the dephasing time T_2^* by a factor of 6.75 for the Si-doped GaAs system. Furthermore, considering the inherent strain environment of our QDs, the noncollinear type of interaction mediated by the quadrupolar moments of the nuclei is expected to play an important role and may increase the influence on T_2^*, see refs. [10,12,14,36].

DISCUSSION

The 1 GHz laser repetition frequency used in this study allows us to explore the electron-nuclear spin dynamics for a pure single-mode Larmor spin precession in the inhomogeneous ensemble of (In,Ga)As/GaAs QDs. This is the first experimental realization of such a situation, which allows us to demonstrate the discretization of the total magnetic field acting on the electron spins. Furthermore, we confirm that at the center of the frequency plateaus, the nuclear spin fluctuations become reduced without build-up of a dynamic nuclear polarization, a situation comparable to the coherent population trapping experiments performed on single quantum dots. The pulsed excitation relaxes the requirement of a strictly accurate spectral tuning of the lasers (as required for a single QD) and makes this technique more universal. Additionally, the suggested two-laser protocol opens up a promising way to establish a reduced nuclear spin fluctuation surrounding using a high repetiton laser oscillator, while the lower repetition laser can be used for readout and manipulation of a large ensemble of spins.

METHODS

Sample

The (In,Ga)As/GaAs QD ensemble was grown by molecular beam epitaxy on a (100)-oriented GaAs substrate. Adjacent sheets in the 20 QD layers are separated by 80 nm wide GaAs barriers. Resident electrons are provided by a δ doping layer of Silicon placed 16 nm above each layer. The sample is thermally annealed at a temperature of 945 °C for 30 s to homogenize the QD size distribution and to shift the average transition energy to 1.39 eV.

Setup

The electron spin polarization is measured at a sample temperature of $T = 5.3$ K using pump-probe spectroscopy in an external magnetic field B_x applied perpendicular to the light propagation (Voigt geometry). Two

lasers are used. The first one is a Ti:Sapphire laser with a pulse duration of 2 ps, a spectral full width at half maximum (FWHM) of 0.9 meV, and a pulse repetition frequency of 75.76 MHz (repetition period of 13.2 ns). The second laser is a Ti:Sapphire laser with a pulse duration of 150 fs and a repetition frequency of 1 GHz (repetition period of 1 ns). The pulses of the 1 GHz laser are spectrally shaped using two sets of holographic gratings and slits (one set for pump and one for probe) to reach about 0.9 meV FWHM (duration of 1.5 ps). The gratings enable us to introduce an energy detuning between the pump and probe beams. Both lasers are not synchronized or phase-locked.

The experiments presented in Fig. 1 and Fig. 3 are carried out using the degenerate case of pump-probe energies and external magnetic fields fixed at the integer precession modes, $B_x = KB_0$. At these magnetic fields, the overall behavior is determined only by the negatively detuned electron transitions and it makes no difference if one uses degenerate or negatively detuned pulses. We found it experimentally easier to implement the degenerate case whenever possible as it requires one parameter less to control. For the experiments presented in Fig. 2, the energy detuning plays an important role as it determines the direction of the Overhauser field while the external magnetic field is varied.

The time-resolved measurements are enabled by mechanical delay lines. To reduce the impact of scattered light, a double modulation scheme is used. The pump is helicity-modulated between left- and right-circular polarization using a photo-elastic modulator with a frequency of 84 kHz. The probe is intensity modulated with a frequency of 100 kHz while being vertically polarized. The signal is measured by a lock-in amplifier using the difference frequency of 16 kHz as a reference. The pump beams of both lasers are sent through the same lens and are focused to a spot diameter of 50 µm. The probe beams are focused to 40 µm spots. In this way, approximately 5×10^5 QDs are excited at the same time. The Faraday rotation of the probe beam is proportional to the electron spin projection along the light propagation direction and is measured using an optical bridge consisting of a Wollaston prism to separate the linear polarizations and Si-based balanced photo diodes.

For the extended version of the pump-probe experiment, we use the 1 GHz laser, where the pump and probe pulses are picked by electro-optical modulators (EOM), hitting the sample in bunches. The pump and probe bunches are separated by an electronically controlled delay. As the devices used here are not fast enough to have a high extinction ratio between neighboring pulses within a nanosecond, the rising and falling edges of the bunches have varying pulse amplitudes within about 6 ns. This time sets a limit on the time resolution of the extended pump-probe and makes it not usable for decay times shorter than 6 ns. The pump and probe pulses stay synchronized to each other and the varying phase of the EOMs relative to the laser repetition frequency mainly add an additional exponential decay proportional to the falling edge of the EOMs used to select the pulse bunches. Here we use 130 pump pulses and six probe pulses for the corresponding bunches. This pump-probe sequence is repeated with a period of 516 ns.

DATA AVAILABILITY

The data that support the findings of this study are available from the corresponding author upon reasonable request.

Received: 5 November 2020; Accepted: 11 March 2021;
Published online: 16 April 2021

REFERENCES

1. Liao, S.-K. et al. Satellite-to-ground quantum key distribution. *Nature* **549**, 43–47 (2017).
2. Arute, F. et al. Quantum supremacy using a programmable superconducting processor. *Nature* **574**, 505–510 (2019).
3. Ladd, T. D. et al. Quantum computers. *Nature* **464**, 45–53 (2010).
4. Merkulov, I. A., Efros, A. L. L. & Rosen, M. Electron spin relaxation by nuclei in semiconductor quantum dots. *Phys. Rev. B* **65**, 205309 (2002).
5. Greilich, A. et al. Mode locking of electron spin coherences in singly charged quantum dots. *Science* **313**, 341–345 (2006).
6. Wüst, G. et al. Role of the electron spin in determining the coherence of the nuclear spins in a quantum dot. *Nat. Nanotechnol.* **11**, 885–889 (2016).
7. Wehner, S., Elkouss, D. & Hanson, R. Quantum internet: a vision for the road ahead. *Science* **362**, 303–312 (2018).
8. Stepanenko, D., Burkard, G., Giedke, G. & Imamoglu, A. Enhancement of electron spin coherence by optical preparation of nuclear spins. *Phys. Rev. Lett.* **96**, 136401 (2006).
9. Xu, X. et al. Optically controlled locking of the nuclear field via coherent dark-state spectroscopy. *Nature* **459**, 1105–1109 (2009).
10. Latta, C. et al. Confluence of resonant laser excitation and bidirectional quantum-dot nuclear-spin polarization. *Nat. Phys.* **5**, 758–763 (2009).
11. Onur, A. R. et al. Stabilizing nuclear spins around semiconductor electrons via the interplay of optical coherent population trapping and dynamic nuclear polarization. *Phys. Rev. B* **93**, 161204 (2016).
12. Éthier-Majcher, G. et al. Improving a solid-state qubit through an engineered mesoscopic environment. *Phys. Rev. Lett.* **119**, 130503 (2017).
13. Bodey, J. H. et al. Optical spin locking of a solid-state qubit. *npj Quantum Inf.* **5**, 95 (2019).
14. Gangloff, D. A. et al. Quantum interface of an electron and a nuclear ensemble. *Science* **364**, 62–66 (2019).
15. Urbaszek, B. et al. Nuclear spin physics in quantum dots: an optical investigation. *Rev. Mod. Phys.* **85**, 79–133 (2013).
16. Bechtold, A. et al. Three-stage decoherence dynamics of an electron spin qubit in an optically active quantum dot. *Nat. Phys.* **11**, 1005–1008 (2015).
17. Greilich, A. et al. Nuclei-induced frequency focusing of electron spin coherence. *Science* **317**, 1896–1899 (2007).
18. Markmann, S., Reichl, C., Wegscheider, W. & Salis, G. Universal nuclear focusing of confined electron spins. *Nat. Commun.* **10**, 1097 (2019).
19. Belykh, V. V. et al. Extended pump-probe faraday rotation spectroscopy of the submicrosecond electron spin dynamics in *n*-type GaAs. *Phys. Rev. B* **94**, 241202 (2016).
20. Greilich, A. et al. Collective single-mode precession of electron spins in an ensemble of singly charged (In,Ga)As/GaAs quantum dots. *Phys. Rev. B* **79**, 201305 (2009).
21. Greilich, A. et al. A way to a single frequency precession of an inhomogeneous ensemble of electron spins in InGaAs quantum dots. *Phys. Status Solidi C* **6**, 428–431 (2009).
22. Yugova, I. A. et al. Exciton fine structure in InGaAs/GaAs quantum dots revisited by pump-probe faraday rotation. *Phys. Rev. B* **75**, 195325 (2007).
23. Yugova, I. A., Glazov, M. M., Ivchenko, E. L. & Efros, A. L. L. Pump-probe faraday rotation and ellipticity in an ensemble of singly charged quantum dots. *Phys. Rev. B* **80**, 104436 (2009).
24. Greilich, A. et al. Optical control of spin coherence in singly charged (In, Ga)As/GaAs quantum dots. *Phys. Rev. Lett.* **96**, 227401 (2006).
25. Evers, E. et al. Decay and revival of electron spin polarization in an ensemble of (In,Ga)As quantum dots. *Phys. Rev. B* **98**, 075309 (2018).
26. Zhukov, E. A. et al. Discretization of the total magnetic field by the nuclear spin bath in fluorine-doped ZnSe. *Nat. Commun.* **9**, 1941 (2018).
27. Carter, S. G. et al. Directing nuclear spin flips in InAs quantum dots using detuned optical pulse trains. *Phys. Rev. Lett.* **102**, 167403 (2009).
28. Korenev, V. L. Multiple stable states of a periodically driven electron spin in a quantum dot using circularly polarized light. *Phys. Rev. B* **83**, 235429 (2011).
29. Abragam, A. *The Principle of Nuclear Magnetism*. (Oxford University Press, Oxford, 1961).
30. Glazov, M. M. *Electron and Nuclear Spin Dynamics in Semiconductor Nanostructures*. (Oxford University Press, Oxford, 2018).
31. Xu, X. et al. Coherent population trapping of an electron spin in a single negatively charged quantum dot. *Nat. Phys.* **4**, 692–695 (2008).
32. Zhukov, E. A. et al. Spin inertia of resident and photoexcited carriers in singly charged quantum dots. *Phys. Rev. B* **98**, 121304 (2018).
33. Gangloff, D. A. et al. Revealing beyond-mean-field correlations in a nuclear ensemble via a proxy qubit. Preprint at http://arxiv.org/abs/2012.11279 (2020).
34. Cohen-Tannoudji, C. & Dupont-Roc, J. Experimental study of Zeeman light shifts in weak magnetic fields. *Phys. Rev. A* **5**, 968–984 (1972).
35. Onur, A. R. & van der Wal, C. H. Two-laser dynamic nuclear polarization with semiconductor electrons: Feedback, suppressed fluctuations, and bistability near two-photon resonance. *Phys. Rev. B* **98**, 165304 (2018).
36. Högele, A. et al. Dynamic nuclear spin polarization in the resonant laser excitation of an ingaas quantum dot. *Phys. Rev. Lett.* **108**, 197403 (2012).

ACKNOWLEDGEMENTS

We are grateful to V.L. Korenev for valuable discussions. We acknowledge the financial support by the Deutsche Forschungsgemeinschaft in the frame of the International Collaborative Research Center TRR 160 (Project A1) and the Russian Foundation for Basic Research (Grant No. 19-52-12059). I.A.Yu. acknowledges the support by Saint-Petersburg State University Research Grant No. 73031758. A.G. acknowledges support by the BMBF-project Q.Link.X (Contract No. 16KIS0857). The AFM figure was provided by Claudia Bock, Ruhr-Universität Bochum.

AUTHOR CONTRIBUTIONS

E.E. and A.G. conceived the experiment. E.E. and N.E.K. carried out the experiment and took the experimental data. E.E., N.E.K. and A.G. analyzed the experimental data. N.E.K. and I.A.Yu. conceived the theoretical model. D.R. and A.D.W. prepared the sample. E.E., N.E.K., I.A.Yu., D.R.Ya., M.B. and A.G. wrote the manuscript.

FUNDING

Open Access funding enabled and organized by Projekt DEAL.

COMPETING INTERESTS

The authors declare no competing interests.

ADDITIONAL INFORMATION

Supplementary information The online version contains supplementary material available at https://doi.org/10.1038/s41534-021-00395-1.

Correspondence and requests for materials should be addressed to E.E.